Postprint of: Warecka M., Lech R., Kowalczyk P., Hybrid Analysis of Structures Composed of Axially Symmetric Objects, IEEE Transactions on Microwave Theory and Techniques,
DOI: 10.1109/TMTT.2020.3014944

Hybrid Analysis of Structures Composed of Axially Symmetric Objects

Malgorzata Warecka, *Graduate Student Member, IEEE*, Rafal Lech, *Senior Member, IEEE*, and Piotr Kowalczyk, *Member, IEEE*

***Abstract*— A hybrid method for the scattering problems in shielded and open structures is presented. The procedure is based on the combination of body-of-revolution involving finite-element methods with impedance matrix formulation and the mode-matching technique, which can be utilized for the analysis of structures with axially symmetrical scatterers. In order to confirm the validity and efficiency of the proposed approach, a few examples of electromagnetic field scattering in open and waveguide structures are analyzed. The results cohere with those obtained by commercial software.**

***Index Terms*— Body of revolution (BOR), cylindrical waveguides, finite-element method (FEM), generalized impedance matrix (GIM), periodic structures, scattering, waveguide discontinuities.**

I. Introduction

SCATTERING and propagation problems are important issues in the analysis and design of microwave, RF, and optical devices (e.g., shaping of radiation patterns, filters, phase shifters, or circulators). There are many different methods for solving such problems. They can be separated in terms of geometrical complexity or divided into analytical and discrete techniques. For simple structures, the analysis can be performed using analytical methods. This provides great accuracy and fast calculations; however, it is associated with an exasperating lack of versatility. They are therefore only used for some structures, such as cylinders, spheres, and ellipsoids. In these cases, the field can be described with the use of the Hankel or Mathieu functions (respectively, for cylindrical and elliptical rods), and the mode-matching method can be utilized [1]–[6]. For slightly more complex structures, a solution can be found with the use of quasi-analytical techniques (for example, the field-matching method), which are more general than the previous ones and are still quite efficient [7], [8]. Nevertheless, they are limited to rods with convex cross sections in 2.5-D problems. There are other techniques that are much more versatile, for example, integral equation methods that involve Green's functions. However, the improvement of versatility comes at a cost—some problems remain and new ones appear. The first issue is the choice of basis functions (similar to the mode- and field-matching methods), and the second is singularities of Green's functions [9]. The most versatile techniques are discrete methods, such as the finite-element or finite-difference (FD) method. In these techniques, there are no geometrical restrictions imposed, and therefore, they are commonly used in commercial software. Nonetheless, they require fine discretization for complex geometries, which affects calculation time and memory requirements. Another issue for these kinds of methods is domain truncation for unshielded structures. Improper truncation affects accuracy; proper truncation may require a number of ambiguous parameters [as in perfectly matched layer (PML)] and expands the computational domain. To combine the advantages of analytical and discrete techniques, hybrid methods have been developed. The analysis is made faster by a proper division of the computational domain while remaining versatile; in some cases, they also eliminate boundary condition issues.

There are many different hybrid methods [10]–[14], but in this article, we will focus on one of the most effective: a combination of the generalized impedance matrix (GIM) and mode-matching method. In this approach, the domain is divided into two regions: an inner and an outer one. In the inner region, which is represented by GIM, a discrete method can be employed, such as the finite-element method (FEM). Utilization of any discrete method permits calculating GIM at the boundary and, using this model, the entire inner part of the domain. In this way, a very arduous discrete method needs to be used only in a small part of the domain. In the outer region, fields are described analytically by a series of fixed basis functions (as in mode- or field-matching methods). For structures with axial symmetry or with at least one element with such symmetry, the discrete part of the analysis can be further improved. This approach is well known in the literature as body of revolution (BOR) and permits a significant reduction of the problem [15]–[28]. There are many geometrical structures that fulfill the condition of axial symmetry, such as cylinders, cones, hourglass shapes, and many others. In these instances, a calculation of GIM does not require

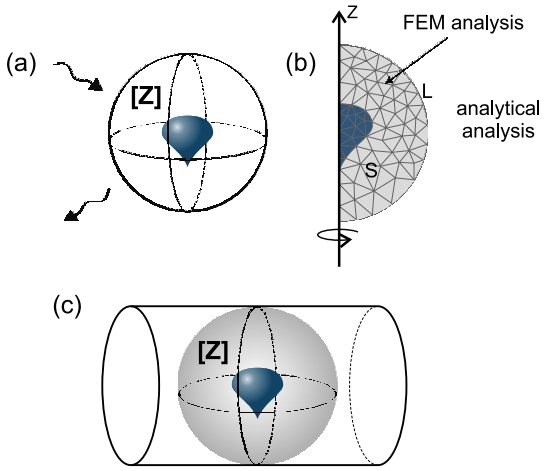

Fig. 1. Schematic views of (a) object illuminated by a plane wave, (b) computational domain, and (c) waveguide with a scatterer.

3-D FEM, but only 2.5-D, which makes the computation more efficient.

In this article, a combination of the FEM with GIM and the mode-matching technique is presented. A mixture of FEM and BOR provides fast determination of GIM and, hence, an effective analysis of the whole structure. A scatterer is surrounded by a semicircular port, which permits an analysis of structures with finite dimensions, as opposed to [29] where infinite cylinders were considered (see Fig. 1). These scatterers can be arbitrarily rotated and placed in waveguides, which makes this method more versatile. The proposed approach is a modification of the technique presented in [10] and [11] where the FD method was used. The discrete part of the proposed approach is based on [30], where axially symmetrical waveguides were analyzed.

Moreover, utilization of FEM instead of FD eliminates the problem of even discretization (used in FD) and permits the use of a sparser mesh. In addition, contrary to FD [10], [11], in FEM, there is no need to employ any effective permittivity or mesh modifications on a metal surface.

This approach also carries great potential for the use of model order reduction in the GIM [31]. In addition, the mesh morphing technique can be utilized [32], which is an undoubted advantage in the context of the design process.

II. Formulation of the Problem

The aim of the analysis is to determine scattering fields in open and closed structures consisting of axially symmetrical objects (see Fig. 1).

In Section II-A, it is shown that the GIM can be used in both closed and open structure analyses, i.e., to determine the scattered field from an object at any known excitation. Any scattering object can be replaced with an artificial object (containing the scatterer) of simple geometry on the surface of which the GIM is defined. In other words, the GIM can be applied to simplify the analysis by changing the complex geometric structure to a simple one. This approach allows for the fields to be analytically described outside the object. In Section II-B, the GIM for a spherical subdomain is defined.

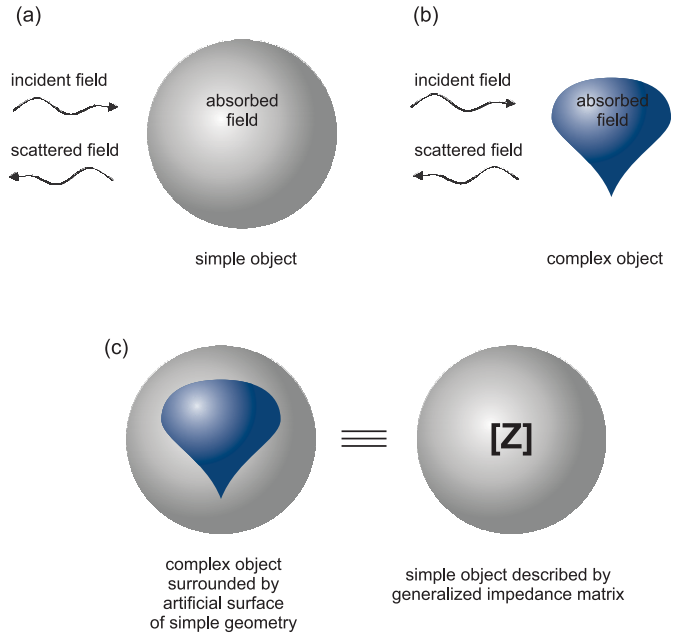

Fig. 2. Idea of simplification involving GIM. (a) Scattering from sphere. (b) Scattering from object with complex geometry. (c) Description of the object by its generalized impedance matrix.

For scattering structures with axial symmetry, the GIM can be determined using FEM with BOR, as shown in Section II-C.

A. Scattering of EM Waves in Open and Closed Structures

The analysis of electromagnetic field scattering from a material object is based on the assumption of a known incident field illuminating the object and searching for an unknown scattered field from that object. In general, the problem can be described by a set of equations (at the boundary of the scatterer)

$$\vec{E}^{\text{inc}} + \vec{E}^{\text{scat}} = \vec{E}^{\text{abs}} \quad (1)$$

$$\vec{H}^{\text{inc}} + \vec{H}^{\text{scat}} = \vec{H}^{\text{abs}} \quad (2)$$

where superscripts *inc* and *scat* refer, respectively, to the incident and the scattered field by the object, and *abs* refers to the absorbed field in the object. If the geometry of the object is simple [see Fig. 2(a)], e.g., a cylinder, an ellipse, or a sphere, the fields, both inside and outside the object, can be described analytically by expansion in series of appropriate functions (depending on the coordinate system used). In this case, the mode-matching method is commonly utilized, which allows for quickly obtainable, accurate results. When the object is of complex geometry [see Fig. 2(b)], the analytical description is difficult or often impossible; therefore, other numerical techniques need to be employed, such as discrete methods, which, while less efficient, are more versatile. However, if the electromagnetic field is calculated in the vicinity of the object, e.g., on the surface of a cylinder or a sphere, surrounding the object, then in further analysis, this artificial surface can replace the object [see Fig. 2(c)]. It is then possible to combine both methods where the discrete method is utilized only within and in the close proximity of the object, while outside the artificial surface, an analytical description can

be used. Such combination is possible by relating electric and magnetic fields on the artificial surface in the form of impedance. In the algorithm, the electric and magnetic fields are projected on the appropriate sets of orthogonal functions and the impedance relation is described with respect to the coefficients of both fields. In this approach, $\vec{E}^{\text{abs}}$ and $\vec{H}^{\text{abs}}$ from (1) and (2) relate to the field inside the artificial object on the surface of which the following relation can be formulated:

$$\mathbf{C}^E = \mathbf{Z}\mathbf{C}^H \tag{3}$$

where $\mathbf{C}^{E,H}$ denote vectors of coefficients of $\vec{E}^{\text{abs}}$ and $\vec{H}^{\text{abs}}$ fields. In order to minimize the computational effort, the discrete domain should be as small as possible, i.e., the surrounding surface should enclose the object in very close proximity. However, due to the possibility of an occurrence of the local singular fields at the sharp edges of the scatterer, the surface cannot be in contact with the object.

Next, utilizing the calculated GIM, a T-matrix on the artificial surface can be easily calculated [10]. The T-matrix relates to the coefficients of incident and scattered fields and with a known excitation allows for the scattered field to be calculated. It is worth noting that such description of the object depends on the geometry and material properties of the object, but is independent of an excitation. Therefore, the analyzed object, which is described by GIM or T-matrix, can be placed in different scenarios, e.g., illuminated by a plane wave while in free space, placed in a waveguide junction and excited by a waveguide field or enclosed by a metallic wall forming a cavity. Such an approach was previously used for the analysis of structures containing inhomogeneous dielectric cylinders [33], cylinders of arbitrary shapes [7], [34], or rotationally symmetrical objects [10], [11] both in closed and open structures.

The algorithm utilized in the described approach can be presented in the form of a flowchart shown in Fig. 3. The first step is to calculate the GIM of the analyzed object. A detailed description of this step is presented in the following. From the GIM, the T-matrix is calculated and object rotation can be performed by a simple multiplication of this matrix by rotation matrices [10] without the need for recalculation of GIM or the T-matrix. Next, the type of analysis is chosen. For open problems, the scattered field in near or far zones is calculated. For closed problems, a scattering matrix of a waveguide junction with the analyzed object is determined. In the case of analysis of filtering structures with multiple sections, cascading formulas for S-matrices are utilized to calculate the scattering parameters of the entire structure.

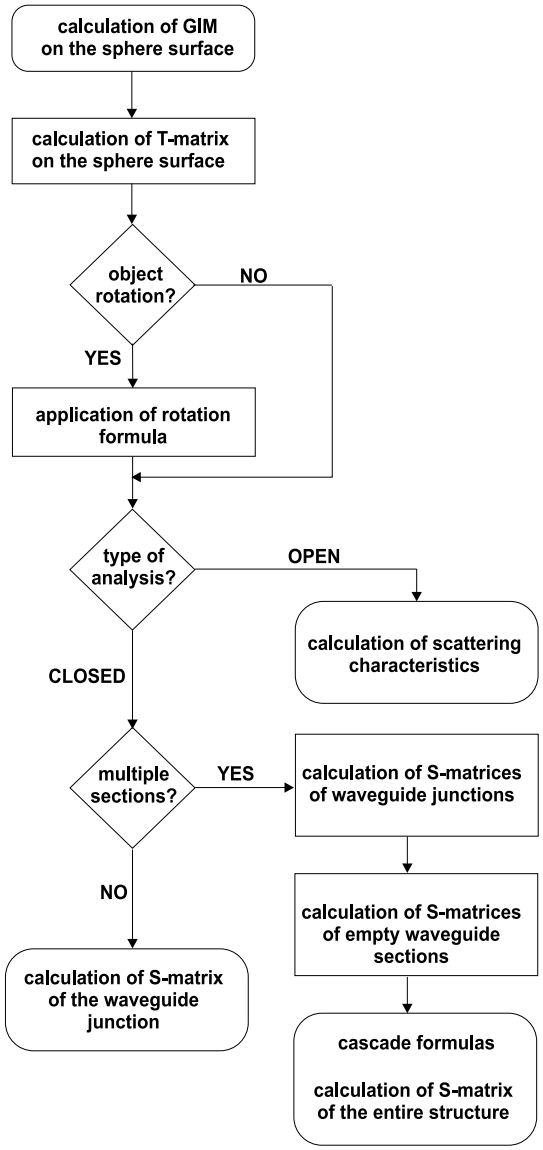

Fig. 3. Flowchart of the algorithm.

B. GIM for a Spherical Subdomain

In the proposed method, a scatterer (or scatterers) is surrounded by a virtual sphere with radius R, on the surface of which the relation between an electric and magnetic field can be defined. This approach permits an analysis of the structure irrespective of excitation (in a limited or an infinite domain) as well as rotation and duplication of the object without repeating the analysis. Assuming basis functions describing the electric $\{\vec{e}^{\text{TE}}_{nm}, \vec{e}^{\text{TM}}_{nm}\}$ and magnetic $\{\vec{h}^{\text{TE}}_{nm}, \vec{h}^{\text{TM}}_{nm}\}$ fields on the aforementioned spherical surface, the relation between the field expansion coefficients in these bases can be obtained [30]. This relation is well known as GIM (denoted as $\mathbf{Z}$)

$$\mathbf{V} = \mathbf{Z}\mathbf{I} \tag{4}$$

where $\mathbf{V} = [\mathbf{V}^{\text{TE}}, \mathbf{V}^{\text{TM}}]$, $\mathbf{I} = [\mathbf{I}^{\text{TE}}, \mathbf{I}^{\text{TM}}]$, and

$$\mathbf{V}^{(\cdot)} = \left[V^{(\cdot)}_{1,-1}, V^{(\cdot)}_{1,0}, V^{(\cdot)}_{1,1}, V^{(\cdot)}_{2,-2}, \ldots, V^{(\cdot)}_{N,N-1}, V^{(\cdot)}_{N,N}\right]^T \tag{5}$$

$$\mathbf{I}^{(\cdot)} = \left[I^{(\cdot)}_{1,-1}, I^{(\cdot)}_{1,0}, I^{(\cdot)}_{1,1}, I^{(\cdot)}_{2,-2}, \ldots, I^{(\cdot)}_{N,N-1}, I^{(\cdot)}_{N,N}\right]^T \tag{6}$$

are vectors containing coefficients of the corresponding electric

$$\vec{E}(R,\theta,\varphi) = \sum_{n=1}^{N}\sum_{m=-n}^{n}\left(V^{\text{TE}}_{nm}\vec{e}^{\text{TE}}_{nm} + V^{\text{TM}}_{nm}\vec{e}^{\text{TM}}_{nm}\right) \tag{7}$$

and magnetic

$$\vec{H}(R,\theta,\varphi) = \sum_{n=1}^{N}\sum_{m=-n}^{n}\left(I^{\text{TE}}_{nm}\vec{h}^{\text{TE}}_{nm} + I^{\text{TM}}_{nm}\vec{h}^{\text{TM}}_{nm}\right) \tag{8}$$

fields, where vector spherical harmonics have been adopted as basis functions $\vec{e}^{\,\mathrm{TM}}_{nm} = \vec{h}^{\,\mathrm{TE}}_{nm} = \vec{N}^{t}_{nm}$ and $\vec{h}^{\,\mathrm{TM}}_{nm} = \vec{e}^{\,\mathrm{TE}}_{nm} = \vec{M}^{t}_{nm}$ and defined as follows:

$$\vec{N}^{t}_{nm} = e^{\mathrm{j}m\varphi}\left(\frac{\partial P^m_n(\cos\theta)}{\partial\theta}\vec{i}_\theta + \frac{\mathrm{j}m}{\sin\theta}P^m_n(\cos\theta)\vec{i}_\varphi\right)$$
$$\vec{M}^{t}_{nm} = e^{\mathrm{j}m\varphi}\left(\frac{\mathrm{j}m}{\sin\theta}P^m_n(\cos\theta)\vec{i}_\theta - \frac{\partial P^m_n(\cos\theta)}{\partial\theta}\vec{i}_\varphi\right).$$

C. Evaluation of GIM Using FEM Combined With BOR

This part of the proposed algorithm is similar to the procedure described in [30] where the waveguides with axial symmetry were analyzed. The main difference is related to the port definition. In [30], two circular ports were introduced at the ends of the waveguide junction, whereas in the proposed procedure, a single spherical port is utilized. The matrix $\mathbf{Z}$ is similar and can be determined using the relation

$$\mathbf{Z} = j\omega\mu_0\mathbf{\Delta}^{-1}\mathbf{B}^H\mathbf{G}^{-1}\mathbf{B} \tag{9}$$

where matrix $\mathbf{G}$ takes exactly the same form as in [30]. However, the matrices $\mathbf{B}$ and Δ need to be changed because they are directly related to boundary conditions. By rewriting fields as a component in the direction φ: $\vec{E}_\varphi(\rho,z) = E_\varphi(\rho,z)\vec{i}_\varphi$ and as a tangential component: $\vec{E}_t(\rho,z) = E_\rho(\rho,z)\vec{i}_\rho + E_z(\rho,z)\vec{i}_z$, a weak form of the wave equation can be written for scalar components as follows:

$$\begin{aligned}
&-\iint_S \frac{jm}{\rho}\mathbf{grad}_t(\rho F_\varphi)\cdot\mu_r^{-1}\vec{E}_t\,d\rho dz \\
&\quad - k_0^2\iint_S \rho F_\varphi\varepsilon_r E_\varphi\,d\rho dz \\
&\quad + \iint_S \frac{1}{\rho}\mathbf{grad}_t(\rho F_\varphi)\cdot\mu_r^{-1}\mathbf{grad}_t(\rho E_\varphi)\,d\rho dz \\
&\quad + 2\pi R^2 j\omega\mu_0\int_L F_\varphi(\vec{i}_\varphi\times\vec{H}_t)\cdot\vec{i}_r\sin\theta d\theta \\
&= 0
\end{aligned} \tag{10}$$

and for vector components

$$\begin{aligned}
&\iint_S \rho\ \mathbf{curl}_t\vec{F}_t\cdot\mu_r^{-1}\mathbf{curl}_t\vec{E}_t\,d\rho dz \\
&\quad - k_0^2\iint_S \rho\vec{F}_t\cdot\varepsilon_r\vec{E}_t\,d\rho dz \\
&\quad + \iint_S \frac{jm}{\rho}\vec{F}_t\cdot\mu_r^{-1}\mathbf{grad}_t(\rho E_\varphi)\,d\rho dz \\
&\quad + \iint_S \frac{m^2}{\rho}\vec{F}_t\cdot\mu_r^{-1}\vec{E}_t\,d\rho dz \\
&\quad + 2\pi R^2 j\omega\mu_0\int_L(\vec{F}_t\times\vec{H}_\varphi)\cdot\vec{i}_r\sin\theta d\theta \\
&= 0
\end{aligned} \tag{11}$$

where

$$\mathbf{curl}_t\vec{A}_t = \vec{i}_\varphi\left(\frac{\partial A_\rho}{\partial z} - \frac{\partial A_z}{\partial\rho}\right)$$
$$\mathbf{grad}_t f = \vec{i}_\rho\frac{\partial f}{\partial\rho} + \vec{i}_z\frac{\partial f}{\partial z}.$$

The relative permittivity and permeability of the structure are represented by ε_r and μ_r, respectively, and k_0 is a vacuum wavenumber. F_φ and $\vec{F}_t$ are testing functions. The computational domain S is represented by a semicircle bounded by L. The magnetic field on the boundary is decomposed and expressed in spherical coordinates as a component in the direction φ: $\vec{H}_\varphi(R,\theta) = H_\varphi(R,\theta)\vec{i}_\varphi$ and the tangential component: $\vec{H}_t(R,\theta) = H_r(R,\theta)\vec{i}_r + H_\theta(R,\theta)\vec{i}_\theta$.

The local matrix $\mathbf{B}$ for each element q (i.e., the element of finite element mesh) is defined as follows:

$$\mathbf{B}^{[q]} = \begin{bmatrix} \mathbf{B}^{[q]}_{t,\mathrm{TE}} & \mathbf{B}^{[q]}_{t,\mathrm{TM}} \\ \mathbf{B}^{[q]}_{\varphi,\mathrm{TE}} & \mathbf{B}^{[q]}_{\varphi,\mathrm{TM}} \end{bmatrix} \tag{12}$$

and its terms take form

$$\begin{aligned}
\left[\mathbf{B}^{[q]}_{t,\mathrm{TE}}\right]_{k,\nu} &= 2\pi R^2\int_L \vec{W}^{[q]}_{(k)}\cdot\left(\vec{i}_r\times\vec{h}^{\,\mathrm{TE}}_{\varphi,nm}\right)\sin\theta\,d\theta \\
\left[\mathbf{B}^{[q]}_{t,\mathrm{TM}}\right]_{k,\nu} &= 2\pi R^2\int_L \vec{W}^{[q]}_{(k)}\cdot\left(\vec{i}_r\times\vec{h}^{\,\mathrm{TM}}_{\varphi,nm}\right)\sin\theta\,d\theta \\
\left[\mathbf{B}^{[q]}_{\varphi,\mathrm{TE}}\right]_{k,\nu} &= 2\pi R^2\int_L \alpha^{[q]}_{(k)}\vec{i}_\varphi\cdot\left(\vec{i}_r\times\vec{h}^{\,\mathrm{TE}}_{t,nm}\right)\sin\theta\,d\theta \\
\left[\mathbf{B}^{[q]}_{\varphi,\mathrm{TM}}\right]_{k,\nu} &= 2\pi R^2\int_L \alpha^{[q]}_{(k)}\vec{i}_\varphi\cdot\left(\vec{i}_r\times\vec{h}^{\,\mathrm{TM}}_{t,nm}\right)\sin\theta\,d\theta
\end{aligned}$$

where $\nu = 1, 2, \ldots, N(N+2)$ corresponds to a specific mode nm by relation $\nu = n^2+3n+m+1$. In the analysis, the standard hierarchical (scalar and vector) basis functions [35] $\alpha^{[q]}_{(\cdot)}$ and $\vec{W}^{[q]}_{(\cdot)}$ of the second order were assumed. The matrix $\mathbf{\Delta}$ is defined as follows:

$$\mathbf{\Delta} = \mathrm{diag}\{\mathbf{\Delta}^{\mathrm{TE}}, \mathbf{\Delta}^{\mathrm{TM}}\} \tag{13}$$

where

$$[\Delta^{\mathrm{TE}}]_{\nu,\nu} = -2\pi R^2\int_L \vec{i}_r\cdot\left(\vec{e}^{\,\mathrm{TE}}_t\times\vec{h}^{\,\mathrm{TE}*}_t\right)\sin\theta\,d\theta \tag{14}$$

$$[\Delta^{\mathrm{TM}}]_{\nu,\nu} = -2\pi R^2\int_L \vec{i}_r\cdot\left(\vec{e}^{\,\mathrm{TM}}_t\times\vec{h}^{\,\mathrm{TM}*}_t\right)\sin\theta\,d\theta. \tag{15}$$

III. Numerical Results

In order to validate the proposed method, a few examples were analyzed (both scattering and propagation problems) and compared to commercial software or the literature. The algorithm was implemented in the MATLAB environment, and all of the tests were performed using an Intel Xenon X5690 3.47 GHz (two processors), 64-GB RAM computer.

The first structure investigated was a cylinder, whose dimensions are presented in Fig. 4 and relative permittivity was assumed to be $\varepsilon_r = 3$. It was located along the x-axis and illuminated by a plane wave propagated along the z-axis and polarized in the y-direction. All calculations were performed at a frequency of 8 GHz, and the number of modes considered in this analysis was $N = 8$. The results presented in Fig. 4 were compared with the hybrid method (a combination of the FD and mode-matching methods) [10] and found to be concordant.

The second considered scatterer was a dielectric cone (see Fig. 5). In this case, the material's parameters were the same as in the aforementioned example and the number of modes was set to $N = 10$. The dimensions of the structure and the scattering characteristics are shown in Fig. 5. The orientation of the scatterer and the plane wave illumination

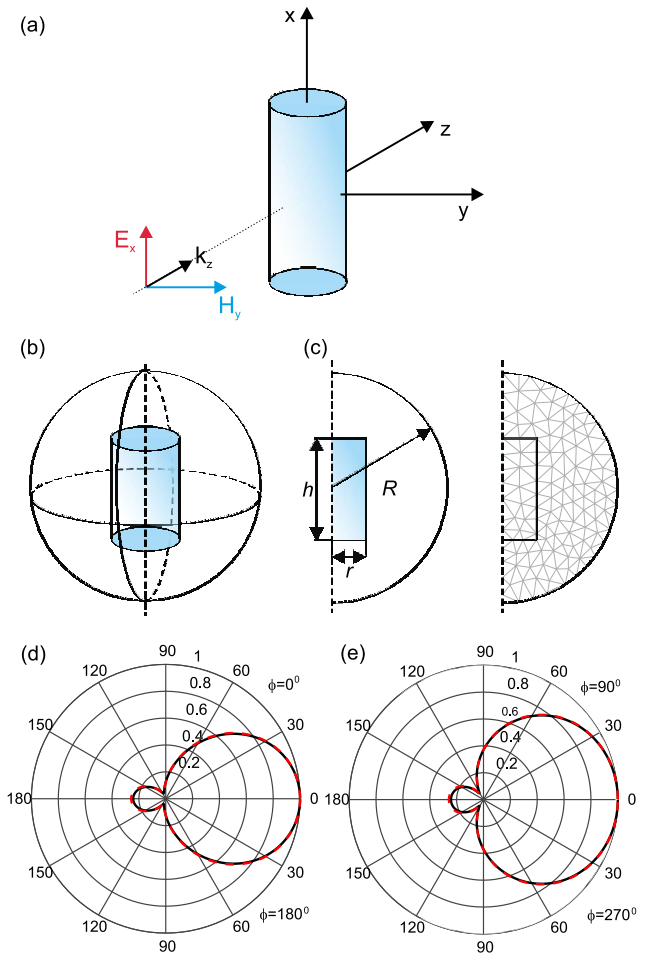

Fig. 4. Plane wave scattering on single dielectric cylinder at (a) plane wave illumination, (b) schematic, and (c) dimensions: $h = 20$ mm, $r = 6$ mm, and $R = 12$ mm; normalized scattered field at frequency 8 GHz in (d) xz plane and (e) yz plane. Solid line: this method. Dashed line: FD/MM method.

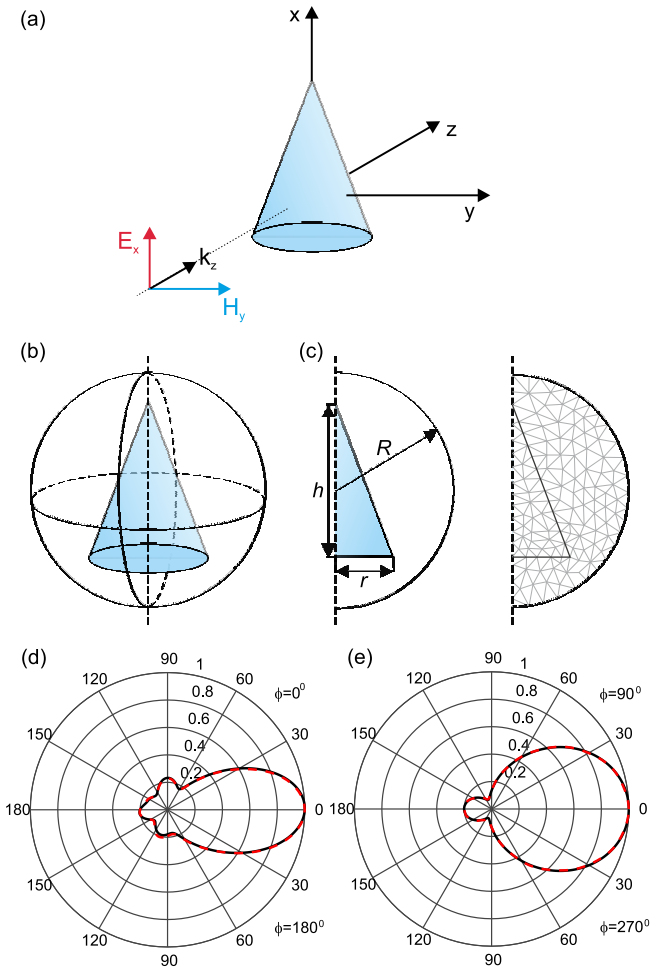

Fig. 5. Plane wave scattering on single dielectric cone at (a) plane wave illumination, (b) schematic, and (c) dimensions: $h = 20$ mm, $r = 6$ mm, and $R = 12$ mm; normalized scattered field at frequency 20 GHz in (d) xz plane and (e) yz plane. Solid line: this method. Dashed line: HFSS.

angle was the same as in the first example. The results were compared with the HFSS commercial software (red dashed line) and a good agreement was achieved.

The third example was a dielectric post in the shape of a dumbbell. As in the previous cases, the relative permittivity was set to $\varepsilon_r = 3$, with the dimensions and results shown in Fig. 6, and the number of modes required for the calculations increased to $N = 15$. The orientation of the scatterer and the plane wave illumination angle was the same as in the previous examples. The results were again compared with HFSS, obtaining good agreement.

In all of the previously presented cases, the total computational time was less than 1 min (including mesh generation, mode matching, and FEM analysis). For comparison, the calculation time of the analysis using the 3-D commercial software (HFSS) was about 1 h (see Table III).

In order to present the application of the method for closed structures, the investigated obstacles were placed in a circular waveguide. The analyzed structure consisted of two metal cylinders ($R = 2.3$ mm and $h = 10$ mm) placed in a waveguide with radius $R = 10$ mm at distance $l_1 = 39$ mm. The scattering parameters were collected and shown in Fig. 7. Both polarizations with respect to the cylinder axis were considered and are denoted by index) along the axis and perpendicular to the cylinder axis. For all obtained results, excellent agreement with commercial software calculations was achieved. The analysis was performed with spherical modes determined by $N = 8$, and waveguide modes were determined by parameter $N_f = 8$ [11]. Such a choice was a consequence of the convergence examination presented in Tables I and II for different distances between the cylinders l_1. The percentage error was evaluated according to the following formula:

$$\delta S_{11} = \frac{\left\| S_{11} - S_{11}^{\mathrm{HFSS}} \right\|}{\left\| S_{11}^{\mathrm{HFSS}} \right\|} \tag{16}$$

where

$$\|S\| = \sqrt{\int_{f_{\min}}^{f_{\max}} |S(f)|^2 df} \tag{17}$$

$f_{\min}$ and $f_{\max}$ define the frequency range, whereas the references were obtained from HFSS simulations.

The next example considers the filtering structure presented in Fig. 8 consisting of a waveguide with radius $R = 10$ mm

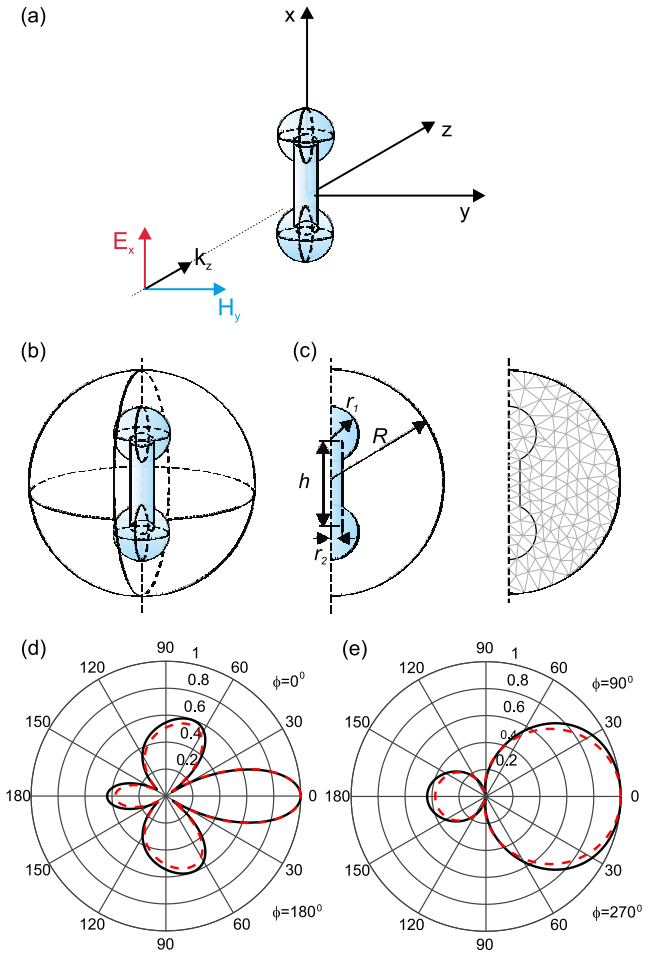

Fig. 6. Plane wave scattering on single dielectric dumbbell at (a) plane wave illumination, (b) schematic view, and (c) dimensions: $r_1 = 3$ mm, $r_2 = 1.5$ mm, $h = 14$ mm, and $R = 12$ mm; normalized scattered field at frequency 20 GHz in (d) xz plane and (e) yz plane. Solid line: this method. Dashed line: HFSS.

TABLE I

PERCENTAGE ERROR δS_{11} OF SCATTERING PARAMETERS FOR STRUCTURE FROM FIG. 7 WITH $l_1 = 19$ mm

N_f	N	number of mesh elements		
		55	110	232
2	2	23.25	22.81	22.72
	4	2.21	1.44	1.27
	6	1.58	0.82	0.65
	8	1.56	0.80	0.64
4	2	37.13	36.77	36.70
	4	1.89	1.12	0.95
	6	1.41	0.66	0.50
	8	1.39	0.64	0.48
6	2	40.85	40.47	40.40
	4	1.87	1.10	0.94
	6	1.41	0.66	0.50
	8	1.39	0.64	0.48
8	2	43.57	43.17	43.10
	4	1.88	1.11	0.94
	6	1.41	0.66	0.50
	8	1.39	0.64	0.48

and three metal cylinders. The dimensions of the middle cylinder were $r = 0.51$ mm and $h = 13.1$ mm and of the two side cylinders, $r = 0.51$ mm and $h = 10.3$ mm. The

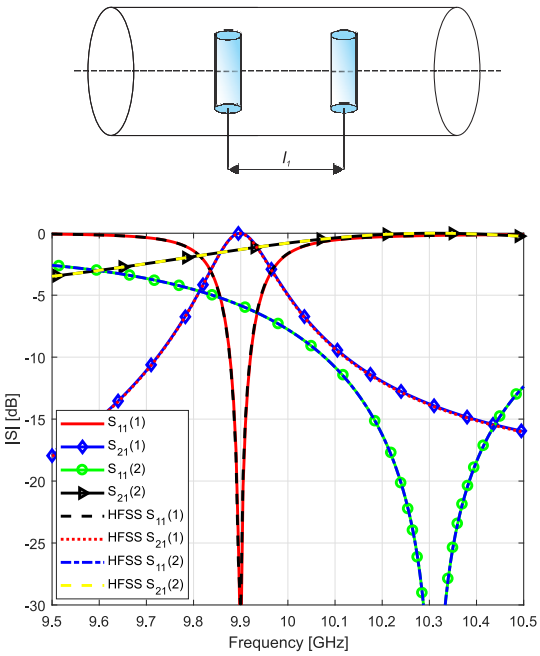

Fig. 7. Schematic of the structure ($l_1 = 39$ mm) and scattering parameters of two metal cylinders placed in a waveguide.

TABLE II

PERCENTAGE ERROR δS_{11} OF SCATTERING PARAMETERS FOR STRUCTURE FROM FIG. 7 WITH $l_1 = 14$ mm

N_f	N	number of mesh elements		
		55	110	232
2	2	9.22	9.09	9.07
	4	1.73	1.23	1.12
	6	1.01	0.52	0.42
	8	1.03	0.54	0.44
4	2	11.75	11.90	11.93
	4	1.22	0.74	0.64
	6	0.90	0.41	0.31
	8	0.89	0.40	0.30
6	2	19.98	19.71	19.66
	4	1.21	0.71	0.60
	6	0.85	0.35	0.25
	8	0.89	0.40	0.30
8	2	13.45	13.30	13.28
	4	1.26	0.76	0.65
	6	0.72	0.28	0.00.22
	8	0.90	0.41	0.31

distance between the cylinder centers was $l_1 = 36$ mm. The scattering parameters of the filter are presented in Fig. 8. The obstacles used in the previous example affected both polarizations as they were both long and thick. The reduction of the obstacle dimensions in one direction allows its influence to be decreased for a chosen wave. Therefore, in this example, the cylindrical posts were very thin that resulted in the complete transmission of perpendicular polarization through the structure.

The computational time of the considered waveguide examples was about ten times shorter than the calculation performed in the 3-D commercial software (see Table III).

As the last example, a periodic structure composed of dielectric cylinders of radius $r = 2.3$ mm, height $h = 10$ mm, and dielectric permittivity $\varepsilon_r = 12$ was calculated. Such

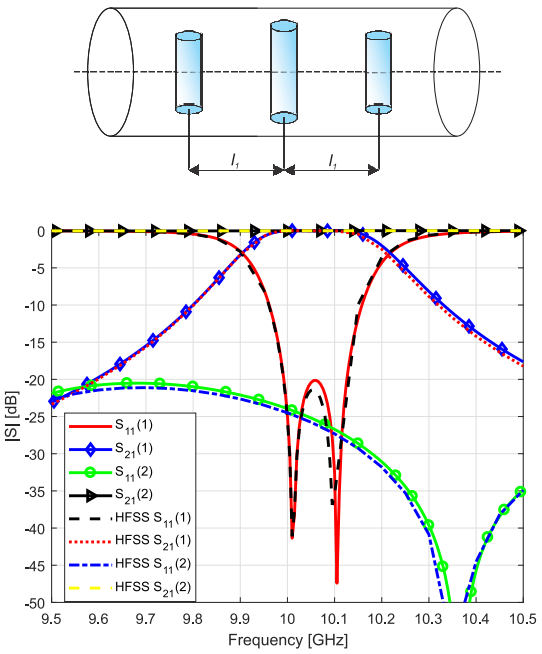

Fig. 8. Schematic of the two-pole filter ($l_1 = 36$ mm) and scattering parameters of the filter.

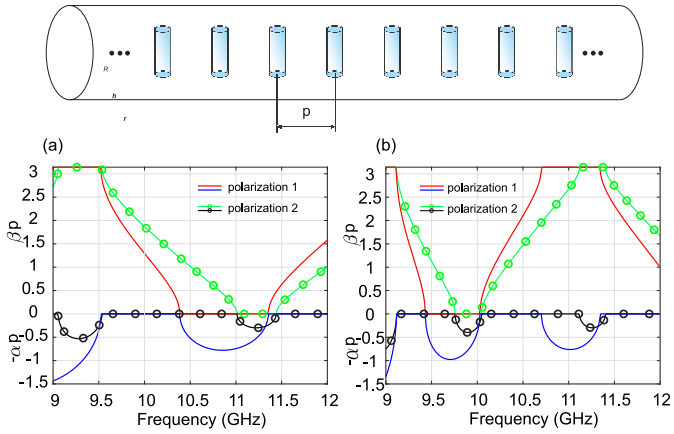

Fig. 9. Normalized propagation coefficients versus frequency for the periodic structure composed of dielectric cylinders with $\varepsilon_r = 12$ of dimensions: $r = 2.3$ mm and $h = 10$ mm. (a) Period $p = 40$ mm. (b) Period $p = 60$ mm.

TABLE III
APPROXIMATED COMPUTATIONAL TIMES

type of structure	our method	HFSS	gain
open structures(Figs. 4 - 6)	1 min	1 h	60 times
filter (Fig. 8)	35 min	6 h	10 times

structures can be analyzed as a cascade connection of a number of waveguide sections of length p (period of the structure) including the investigated objects and described by a scattering matrix. However, the result will describe only a pseudoperiodic structure. Utilizing a formula described in [36], it is possible to calculate propagation coefficients $\gamma = \alpha + j\beta$, with α and β denoting the attenuation and phase coefficients, respectively. The results for the structures with a different period p and for both orthogonal polarizations of fundamental mode are shown in Fig. 9. By changing either period, the dimension, or the shape of the inclusion, it is possible to create a structure with specific passbands and stopbands.

IV. CONCLUSION

A hybrid technique was utilized to investigate structures containing axially symmetrical scatterers. The utilization of BOR and GIM significantly improves the efficiency of the discrete analysis, reducing the computational time by at least an order of magnitude. BOR allows 2.5-D FEM to be utilized for the analysis of a 3-D structure, and GIM is particularly useful in optimization procedures when many identical objects with arbitrary rotation are being investigated (as the rotated and replicated objects do not need FEM recalculation). The proposed approach can also be applied to study periodic/quasi-periodic structures as well as whole devices composed of different waveguide sections. The validity and efficiency of the presented technique have been verified, which confirms its usefulness for the design and optimization process.

REFERENCES

[1] K. Harumi, "Scattering of plane waves by a rigid ribbon in a solid," *J. Appl. Phys.*, vol. 32, no. 8, pp. 1488–1497, Aug. 1961.
[2] E. D. Nielsen, "Scattering by a cylindrical post of complex permittivity in a waveguide," *IEEE Trans. Microw. Theory Techn.*, vol. 17, no. 3, pp. 148–153, Mar. 1969.
[3] J. J. Bowman, T. B. A. Senior, and P. L. E. Uslenghi, *Electromagnetic Scattering by Simple Shapes*. New York, NY, USA: Hemisphere Publishing Corporation, 1969, pp. 349–588.
[4] R. Gesche and N. Lochel, "Scattering by a lossy dielectric cylinder in a rectangular waveguide," *IEEE Trans. Microw. Theory Techn.*, vol. 36, no. 1, pp. 137–144, Jan. 1988.
[5] L. Tsang, J. A. Kong, and K.-H. Ding, *Scattering of Electromagnetic Waves: Theories and Applications*, vol. 27. Hoboken, NJ, USA: Wiley, 2004.
[6] F. G. Mitri, "Acoustic backscattering and radiation force on a rigid elliptical cylinder in plane progressive waves," *Ultrasonics*, vol. 66, pp. 27–33, Mar. 2016.
[7] R. Lech, P. Kowalczyk, and A. Kusiek, "Scattering from a cylindrical object of arbitrary cross section with the use of field matching method," *IEEE Trans. Antennas Propag.*, vol. 64, no. 11, pp. 4883–4887, Nov. 2016.
[8] M. Warecka, R. Lech, and P. Kowalczyk, "Propagation in the open cylindrical guide of arbitrary cross section with the use of field matching method," *IEEE Trans. Antennas Propag.*, vol. 66, no. 6, pp. 3237–3240, Jun. 2018.
[9] W. C. Gibson, *The Method of Moments in Electromagnetics*. Boca Raton, FL, USA: CRC Press, 2014.
[10] A. Kusiek and J. Mazur, "Hybrid finite-difference/mode-matching method for analysis of scattering from arbitrary configuration of rotationally-symmetrical posts," *Prog. Electromagn. Res.*, vol. 110, pp. 23–42, 2010.
[11] A. Kusiek, "Hybrid technique for the analysis of circular waveguide junctions loaded with ferrite posts," *IET Microw., Antennas Propag.*, vol. 9, no. 8, pp. 781–787, Mar. 2015.
[12] J. Rubio, M. A. González, and J. Zapata, "Analysis of open-ended radiating structures based on sfelp (segmentation approach/finite elements/Lanczos-Pade)," in *Proc. IEEE Antennas Propag. Soc. Int. Symp.*, vol. 4, Jun. 2002, pp. 702–705.
[13] J. Rubio, J. Arroyo, and J. Zapata, "Analysis of passive microwave circuits by using a hybrid 2-D and 3-D finite-element mode-matching method," *IEEE Trans. Microw. Theory Techn.*, vol. 47, no. 9, pp. 1746–1749, Sep. 1999.
[14] L. Kuhler, N. Raveu, G. Le Fur, and L. Duchesne, "The modal expansion theory applied TO 3-D metamaterial waveguides characterization," *Prog. Electromagn. Res. M*, vol. 92, pp. 31–41, 2020.
[15] M.-S. Tong, R. Sauleau, A. Rolland, and T.-G. Chang, "Analysis of electromagnetic band-gap waveguide structures using body-of-revolution finite-difference time-domain method," *Microw. Opt. Technol. Lett.*, vol. 49, no. 9, pp. 2201–2206, 2007.

[16] M. Celuch and W. Gwarek, "Industrial design of axisymmetrical devices using a customized FDTD solver from RF to optical frequency bands [Application Notes]," *IEEE Microw. Mag.*, vol. 9, no. 6, pp. 150–159, Dec. 2008.
[17] D.-Y. Na, B.-H.-V. Borges, and F. L. Teixeira, "Finite element time-domain body-of-revolution maxwell solver based on discrete exterior calculus," *J. Comput. Phys.*, vol. 376, pp. 249–275, Jan. 2019.
[18] G. G. Gentili, M. Khosronejad, R. Nesti, G. Pelosi, and S. Selleri, "An efficient 2.5-D finite-element approach based on transformation optics for the analysis of elliptical horns," *IEEE Trans. Antennas Propag.*, vol. 66, no. 9, pp. 4782–4790, Sep. 2018.
[19] G. G. Gentili, G. Macchiarella, and M. Politi, "Modeling of cylindrical dielectric resonator filters by a 2D radial FEM approach," in *Proc. 34th Eur. Microw. Conf.*, vol. 2, Oct. 2004, pp. 593–596.
[20] A. D. Greenwood and J.-M. Jin, "Finite-element analysis of complex axisymmetric radiating structures," *IEEE Trans. Antennas Propag.*, vol. 47, no. 8, pp. 1260–1266, Aug. 1999.
[21] E. A. Dunn, J.-K. Byun, E. D. Branch, and J.-M. Jin, "Numerical simulation of BOR scattering and radiation using a higher order FEM," *IEEE Trans. Antennas Propag.*, vol. 54, no. 3, pp. 945–952, Mar. 2006.
[22] G. G. Gentili, P. Bolli, R. Nesti, G. Pelosi, and L. Toso, "High-order FEM mode matching analysis of circular horns with rotationally symmetric dielectrics," *IEEE Trans. Antennas Propag.*, vol. 55, no. 10, pp. 2915–2918, Oct. 2007.
[23] J.-M. Jin, Z. Lou, Y.-J. Li, N. W. Riley, and D. J. Riley, "Finite element analysis of complex antennas and arrays," *IEEE Trans. Antennas Propag.*, vol. 56, no. 8, pp. 2222–2240, Aug. 2008.
[24] M. M. Ilic, A. Z. Ilic, and B. M. Notaros, "Continuously inhomogeneous higher order finite elements for 3-D electromagnetic analysis," *IEEE Trans. Antennas Propag.*, vol. 57, no. 9, pp. 2798–2803, Sep. 2009.
[25] X. Rui, J. Hu, and Q. H. Liu, "Higher order finite element method for inhomogeneous axisymmetric resonators," *Prog. Electromagn. Res.*, vol. 21, pp. 189–201, 2010.
[26] Y. B. Zhai *et al.*, "Fast computations to electromagnetic scattering properties of complex bodies of revolution buried and partly buried in layered lossy media," *IEEE Trans. Geosci. Remote Sens.*, vol. 49, no. 4, pp. 1431–1440, Apr. 2011.
[27] G. G. Gentili, M. Khosronejad, G. Pelosi, and S. Selleri, "Analysis of elliptical structures with constant axial ratio by body-of-revolution finite element method and transformation optics," *Int. J. Microw. Wireless Technol.*, vol. 11, nos. 5–6, pp. 501–508, Jun. 2019.
[28] J.-M. Jin, *The Finite Element Method in Electromagnetics*. Hoboken, NJ, USA: Wiley, 2015.
[29] P. Kowalczyk, R. Lech, M. Warecka, and A. Kusiek, "Electromagnetic plane wave scattering from a cylindrical object with an arbitrary cross section using a hybrid technique," *J. Electromagn. Waves Appl.*, vol. 33, no. 2, pp. 178–192, Jan. 2019.
[30] M. Warecka, R. Lech, and P. Kowalczyk, "Efficient finite element analysis of axially symmetrical waveguides and waveguide discontinuities," *IEEE Trans. Microw. Theory Techn.*, vol. 67, no. 11, pp. 4291–4297, Nov. 2019.
[31] G. Fotyga, D. Szypulski, R. Lech, and P. Kowalczyk, "Model-order reduction in hybrid methods involving generalized impedance matrix," *IEEE Trans. Antennas Propag.*, vol. 68, no. 8, pp. 6467–6472, Aug. 2020.
[32] M. Czarniewska, G. Fotyga, A. Lamecki, and M. Mrozowski, "Parametrized local reduced-order models with compressed projection basis for fast parameter-dependent finite-element analysis," *IEEE Trans. Microw. Theory Techn.*, vol. 66, no. 8, pp. 3656–3667, Aug. 2018.
[33] M. Polewski, R. Lech, and J. Mazur, "Rigorous modal analysis of structures containing inhomogeneous dielectric cylinders," *IEEE Trans. Microw. Theory Techn.*, vol. 52, no. 5, pp. 1508–1516, May 2004.
[34] A. Kusiek, R. Lech, and J. Mazur, "A new hybrid method for analysis of scattering from arbitrary configuration of cylindrical objects," *IEEE Trans. Antennas Propag.*, vol. 56, no. 6, pp. 1725–1733, Jun. 2008.
[35] D. B. Davidson, *Computational Electromagnetics for RF and Microwave Engineering*. Cambridge, U.K.: Cambridge Univ. Press, 2005.
[36] R. Lech and J. Mazur, "Propagation in rectangular waveguides periodically loaded with cylindrical posts," *IEEE Microw. Wireless Compon. Lett.*, vol. 14, no. 4, pp. 177–179, Apr. 2004.

Malgorzata Warecka (Graduate Student Member, IEEE) received the M.Sc.E.E. degree from the Gdansk University of Technology, Gdansk, Poland, in 2018, where she is currently pursuing the Ph.D. degree.

She is also with the Department of Microwave and Antenna Engineering, Faculty of Electronics, Telecommunications and Informatics, Gdansk University of Technology. Her current research interests include scattering and propagation of electromagnetic wave problems, algorithms, and numerical methods.

Rafal Lech (Senior Member, IEEE) was born in Elblag, Poland, in 1977. He received the M.Sc.E.E., Ph.D. (Hons.), and D.Sc. degrees from the Gdansk University of Technology, Gdansk, Poland, in 2001, 2007, and 2018, respectively.

He is currently with the Department of Microwave and Antenna Engineering, Faculty of Electronics, Telecommunications and Informatics, Gdansk University of Technology. His main research interests are electromagnetic wave scattering, hybrid methods, filter design, complex materials, metamaterial applications at microwave frequencies, electromagnetic analysis of periodic structures, and antenna design.

Piotr Kowalczyk (Member, IEEE) was born in Wejherowo, Poland, in 1977. He received the M.Sc.E.E. degree in applied physics and mathematics and the Ph.D. (Hons.) and D.Sc. degrees in electrical engineering from the Gdansk University of Technology, Gdansk, Poland, in 2001, 2008, and 2018, respectively.

He is currently with the Department of Microwave and Antenna Engineering, Faculty of Electronics, Telecommunications and Informatics, Gdansk University of Technology. His current research interests include scattering and propagation of electromagnetic wave problems, algorithms, and numerical methods.